Targeted intradermal delivery of alpha-arbutin-loaded dissolving polymeric microneedles visualized by three-dimensional Orbitrap secondary ion mass spectrometry (3D OrbiSIMS)

Zhiwei Li [a, b], Maria Marlow[a], David Scurr[a], Zheying Zhu[a]*

a. School of Pharmacy, The University of Nottingham, Nottingham, NG7 2RD, United Kingdom

b. HBN Research Institute and Biological Laboratory, Shenzhen Hujia Technology Co., Ltd., 518000, Shenzhen, Guangdong, P.R. China.

*Corresponding author: Zheying.zhu@nottingham.ac.uk

ABSTRACT

Hyperpigmentation, a prevalent dermatological condition characterized by melanin overproduction, poses treatment challenges due to the hydrophilicity of alpha-arbutin, a widely utilized tyrosinase inhibitor. This study investigates the efficacy of dissolving microneedles (DMNs) in augmenting skin permeation for alpha-arbutin delivery to the targeted epidermal site.

Porcine full-thickness skin was employed in a 24-hour Franz cell study, commencing with the assessment of commercial alpha-arbutin-containing products. Solid steel microneedles (CMNs) from Dermapen® were utilized as both pre- and post-treatment modalities to evaluate the influence of different applications on alpha-arbutin delivery. Additionally, alpha-arbutin-loaded

polyvinylpyrrolidone-co-vinyl acetate (PVPVA) DMNs, containing 2% w/w alpha-arbutin, were fabricated and examined for their permeation-enhancing capabilities. HPLC analysis and 3D Orbitrap Secondary Ion Mass Spectrometry (OrbiSIMS) were employed to quantify and visualize alpha-arbutin in various Franz cell components.

Results indicate that alpha-arbutin permeation to the skin was restricted (less than 1%) without microneedle application and significantly increased by 6-fold (4-5%) with post-treatment CMNs and DMNs, but not with pre-treatment CMNs. Notably, DMNs exhibited a more sustainable and robust capacity than post-treatment CMNs. OrbiSIMS imaging analysis revealed that DMNs visually enhance skin permeation of alpha-arbutin by delivering the compound to the basal layer of the targeted skin location. Overall, this study underscores the potential of DMNs as a promising delivery system for promoting targeted intradermal delivery of alpha-arbutin, providing a comprehensive exploration of various methodologies to identify innovative and improved microneedle approaches for alpha-arbutin permeation.

Keywords: *Intradermal delivery, Hyperpigmentation, Alpha-arbutin, Microneedle, 3D OrbiSIMS, Skin permeation*

Abbreviations: HPLC, High Performance Liquid Chromatography; OrbiSIMS, Orbitrap Secondary Ion Mass Spectrometry; MNs, Microneedles, HA, Ordinary® Alpha- Arbutin 2% + Hyaluronic Acid; AA, Ordinary® Ascorbic Acid 8% + Alpha-Arbutin 2%; INK, The INKEY® List 2% Alpha-Arbutin Serum; OT, object temperature; CT, chamber temperature; CMNs, Commercial Microneedles; DMNs, Dissolving microneedles; PDMS, Polydimethylsiloxane; PVPVA, polyvinylpyrrolidone-co-vinyl acetate; BBC, Basal cell carcinoma

Graphical Abstract

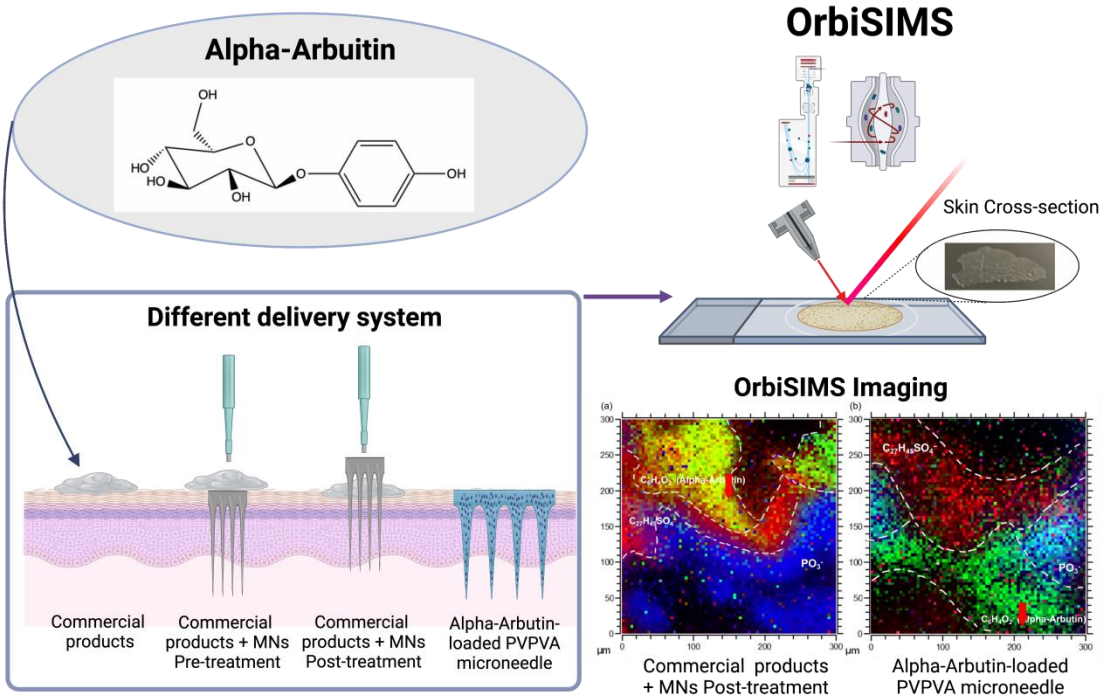

1. Introduction

Melanin, the primary pigment in skin, eyes, and hair, serves as a vital shield with diverse properties. It plays a crucial role in protecting against harmful ultraviolet radiation, acting as a broad-spectrum absorbent, antioxidant, and radical scavenger[1]. It also protects the skin against stress from different sources, including environmental pollutants, toxic drugs, and chemicals. Despite its protective function, an abnormal increase in melanin production results in various hyperpigmentation disorders, such as melasma, postinflammatory hyperpigmentation, solar lentigines, ephelides, and macules[2]. These conditions are generally not harmful but can have a considerable psychological effect on the affected patients due to the effect on their physical appearance[3].

In general, skin disorders are caused by several intrinsic and extrinsic factors, including ultraviolet radiation, radicals, inflammatory mediators, and hormones[4], leading to the upregulation of melanogenesis. Several approaches to achieve depigmentation include regulation of the transcription and activity of tyrosinase, tyrosinase-related protein-1, tyrosinase-related protein-2, and peroxidase, as well as regulation of the uptake and distribution of melanosomes in recipient keratinocytes, regulation of the degradation of melanin and melanosomes, and the turnover of pigmented keratinocytes[5]. Current hyperpigmentation treatments encompass topical agents, chemical peels, cryotherapy, and light or laser therapy[6]. Approximately 15% of the world’s population is estimated to be using depigmenting products[7]. Among them, alpha-arbutin is a widely-used

commercial ingredient, acts as a reversible tyrosinase inhibitor with the IUPAC name (2R,3S,4S,5R,6S)-2 hydroxymethyl-6-(4-hydroxyphenoxy) oxane-3,4,5-triol, aiding in improving skin pigmentation[8]. It inhibits the synthesis of melanin in patients with hyperactive melanocytes and hyperpigmentation disorders. The main mechanism of action of alpha-arbutin is through inhibition of melanosomal tyrosinase activity directly or by competing with the substrate on the active site of the enzyme tyrosinase.

As hyperpigmentation treatment is typically administered topically, successful delivery requires the drug to penetrate the skin's stratum corneum. Corneocytes, constituting the main barrier, possess an insoluble keratin matrix that hinders the diffusion of hydrophilic molecules.[9–11]. The lipophilicity of a drug, measured by its log P value, influences skin permeation. Substances with a log P greater than 2 typically permeate the skin effectively[12]. Despite this, alpha-arbutin, being hydrophilic with a log P of –1.49[13], faces challenges in skin permeation[14]. Moreover, the target site for alpha-arbutin is the basal layer containing melanocytes. This underscores the need for innovative delivery methods to enhance alpha-arbutin's efficacy in treating hyperpigmentation disorders.

Although there are other depigmenting agents with better active effects, alpha-arbutin has a much lower toxic effect profile and does not cause serious adverse effects with long-term exposure[14]. Therefore, it is crucial to improve the permeation of alpha-arbutin across the skin. This can be done by developing novel delivery systems such as microneedles[15], nanosystems[16],

microsystems[17,18], lipidic systems[19], and more[14]. Among these, microneedle technology has been widely explored for improving the skin permeation ability of intradermal and transdermal delivery systems of hydrophilic molecules[20]. Donnelly et al.[21] used solid microneedles to enhance the skin permeation of the hydrophilic compound ALA and to reduce the amount of ALA used. Oh et al.[22] found that biocompatible polycarbonate (PC) microneedles enhance the skin permeation of calcein, a hydrophilic molecule, and thus, they believe it is a suitable tool for transdermal drug delivery systems for hydrophilic molecules.

Microneedles are arrays of microsized projections with lengths ranging from 250 μm to 1000 μm that pierce the skin to create microchannels through the stratum corneum to deliver drug molecules to the target site in the skin[23]. Microneedles can be categorized into five main groups: solid, coated, dissolving, hollow, and hydrogel-forming microneedles[24].

The solid microneedle is normally used for skin pretreatment based on the "poke-and-patch" technique[25]. The needle tips penetrate into the skin, forming microchannels through which the drug directly enters the skin layers upon the application of a drug patch, thus increasing skin permeation[26]. However, the closure of microchannels created after microneedle insertion is a critical aspect when evaluating microneedles, as it influences the drug diffusion rate to the skin microvasculature and interstitial fluid. In a previous study by S Bal.[27], the microchannels generated after solid microneedle application were shown to close

very rapidly - after 15 minutes in most cases[27]. Currently, no study has been carried out to investigate the effectiveness of commercial microneedles (CMNs) in improving the skin permeation of alpha-arbutin. Therefore, commercial solid stainless steel microneedles were used in this study not only as a pretreatment but also as a skin posttreatment based on the "coat-and-poke" technique with slight modifications[28]. The drug was first applied to the skin surface, followed by microneedle insertion. This was to overcome the transient period of microchannel opening for more effective transportation of alpha-arbutin across the skin[29].

In addition to commercial solid microneedles, dissolving microneedle patches are now becoming more mainstream. One major advantage of dissolving microneedles is their ability to improve patient compliance. Dissolving microneedles are typically fabricated using hydrophilic polymers (e.g., PVA or PVP) and by incorporating drug molecules either in solution or nano/microparticle suspension at the casting stage[30,31]. Upon insertion of the dissolving microneedle in the skin, dissolution takes place, and the drug is released into the skin. This is a single-step process without the need for the microneedle to be removed after insertion. Therefore, it is one of the best choices for long-term therapy, as it can improve patient compliance[32].

Recently, Aung et al. developed alpha-arbutin-loaded dissolving microneedles and hydrogel-forming microneedles using polyvinyl alcohol (PVA) and poly(acrylic acid-co-maleic-acid) copolymer (PAMA)[33]. The results were promising, as the dissolving microneedles and hydrogel-forming microneedles showed 4.5 times

and 2.8 times increases in the permeation of alpha-arbutin, respectively, compared to the commercial gel and cream[34]. These data suggest that the dissolving microneedle and hydrogel-forming microneedle offer superior intradermal delivery of alpha-arbutin. However, further attempts to improve targeted delivery by dissolving microneedles through different polymer (e.g., PVPVA) formulations are necessary.

Previous studies have only focused on the total amount of drug delivered into the skin by microneedles, neglecting the specific location. As melanocytes are located between the epidermis and the dermis, if the drug stays only in the upper epidermis, it will not reach the target location. Therefore, a good microneedle system ideally would be capable of delivering the drug to a more precise target site.

To find an optimized microneedle delivery system, the latest OrbiSIMS imaging technique was applied to visualize locations of permeated alpha-arbutin in the skin, together with HPLC quantitative analysis in this study. Although HPLC analysis provides useful quantitative results, this analytical technique does not confer any detail regarding the distribution of alpha-arbutin within individual layers of skin. Hence, additional visual analytical techniques must be explored to provide spatial detail regarding alpha-arbutin permeation. Previously, time-of-flight secondary ion mass spectrometry (ToF-SIMS) has been widely used as a tool for imaging drug spatial distribution in skin layers[28,35,36]. Recently, it has been noted that the incorporation of Orbitrap into ToF-SIMS, also known as 3D OrbiSIMS, has been shown to provide higher mass-resolution capabilities[37], allowing visual analysis

to act as a powerful complementary technique[38]. 3D OrbiSIMS combines the high speed and spatial resolution of secondary ion mass spectrometry (SIMS; under 200 nm for inorganics and under 2 μm for biomolecules) with the high mass resolving power of an Orbitrap (>240,000 at m/z 200)[39]. OrbiSIMS also yields significantly more and stronger peaks than ToF-SIMS, which greatly facilitates further analysis[40]. However, there is still a knowledge gap regarding OrbiSIMS as a visual analysis tool for skin, as its application to skin so far has only been investigated in our recent publication[41]. Thus, this study will be the first to apply 3D OrbiSIMS for visualization of the distribution of alpha-arbutin in the skin, bearing many advantages, including subcellular resolution and no need for radiolabelling or fluorescent labels.

Overall, this study aims to evaluate the skin permeation of commercial alpha-arbutin products and investigate the effects of commercial solid stainless-steel microneedles and polymeric dissolving microneedles (DMNs) on improving the permeation of alpha-arbutin to the target site in the skin, which is visualized and confirmed by OrbiSIMS. Thus, it is suggested that the newly developed DMNs can be used as a promising delivery system to facilitate targeted intradermal delivery of alpha-arbutin for optimal efficacy in the treatment of hyperpigmentation disorders.

2. Materials and methods

2.1. Materials

Deciem Beauty Group Inc. provided Ordinary® Alpha-Arbutin 2% coupled with Hyaluronic Acid and Ordinary® Alpha-Arbutin 2% mixed with 8% Ascorbic Acid. The INKEY List supplied INKEY® Alpha-Arbutin Serum at 2%. Alpha-arbutin pure reference substance, sodium acetate, Kollisolv® PEG400, and glycerine were procured from Merck Life Sciences in the UK. Phosphate saline buffered to pH 7.4, acetic acid, methanol of HPLC purity, Hypersil BDS C18 column of dimensions 150 mm x 4.6 mm ID, and 3.0 µm particles, along with UltiMate™ 3000 HPLC systems, Teepol® cleansing agent and high viscosity sodium carboxymethylcellulose, were acquired from Scientific Laboratory Supplies in the UK. Adhesive sampling discs from D-Squame were ordered through CUDERM Corporation in the USA. The PURELAB® Ultra system from ELGA in the UK was the source of our ultra-purified water. An Eppendorf UK Limited's Centrifuge 5417R was also employed. All chemicals were of analytical caliber, except where noted.

The microneedling instrument, Dermapen®, came from ZJchao in China, designed with cone-shaped microneedles, 370 µm at the base tapering to a 53.4 µm tip. Their pitch measured 620 µm. The selected microneedle length for permeation investigations was 1000 µm, with an oscillation rate of 8000 RPM. Teoxy Beauty, Wuhan, China, was the source for Dermastamp™, a microneedle stamp device. PVPVA Kollidon® of vinyl acetate 64 with a molecular weight between 15-20 kDa was a generous donation from BASF in Germany. OCT embedding medium was obtained from VWR International Ltd., Belgium.

2.2. Fabrication of alpha-arbutin-loaded polyvinylpyrrolidone-co-vinyl acetate (PVPVA) microneedles

The alpha-arbutin infused PVPVA microneedle array was crafted using PDMS templates as per the protocol by Sabri et al[28]. Moulds were composed of 10 x 10 obelisk structures, each measuring 300 µm by 300 µm at the base and reaching a height of 1000 µm, spaced 800 µm apart. The microneedle base was produced by dissolving 16.2% PVPVA by weight per volume and 2% PEG 400 by volume in ultra-purified water, followed by compression for 60 minutes. Subsequently, alpha-arbutin was incorporated into the mix at 2% by weight, after which the blend was evacuated of air for half an hour in a vacuum oven. Next, 150 µl of the mixture was transferred into each mould using precision pipettes and then spun at 4000 RPM for a quarter-hour to occupy the mould cavities completely. The excess was then skimmed off, and the formations were left to dry in a desiccator until the following day.

For the supporting layer, 5.2% weight per weight CMC in ultra-purified water was prepared with constant stirring at 75 °C for 120 minutes, after which glycerol was added at 0.66% volume per weight as a plasticizer. This mixture, amounting to 200 µl, was layered over the needles, followed by centrifugation at 3500 RPM for 10 minutes. The entire set-up was then left to desiccate at room temperature for two days. The microneedles were carefully extracted from their moulds and kept in a desiccator for subsequent use.

Micrographs of the microneedles were taken with a Zeiss Axioplan optical microscope and FEI Quanta 650 ESEM in a low vacuum setting for a precise view of the microneedles' configurations and dimensions. Prior to ESEM analysis, the microneedles were affixed to a metal stage using conductive carbon tape.

2.3. Permeation study of alpha-arbutin through porcine skin

Porcine skin (ear, origin from England) no older than 6 months was acquired from regional slaughterhouses and maintained at 4 $^{\circ}$ C for no longer than a day. The samples were only rinsed with ultra-purified water, with follicles clipped short, and excess fat trimmed away before being wrapped in aluminium foil and frozen at -20 $^{\circ}$ C for no more than 30 days. We utilized the entire thickness of the skin to maintain its native biomechanical characteristics for the Franz cell diffusion tests.

Skin sections were warmed to ambient temperature for at least 60 minutes before the experiment. Round skin sections were then fixed within Franz diffusion cells with the dermal layer facing the lower chamber, exposing an area of 0.64 cm^2 to a 3 mL receiver compartment[42]. The samples were positioned above the receptor section for 15 minutes to reach equilibrium. The integrity of each sample was confirmed through resistance measurement following the method by Davies[43]., only using specimens with resistance over 10 kΩ. The recipient solution was PBS with a pH of 7.4, and temperature during the experiments was consistently held at 33 $^{\circ}$ C, for up to a day.

Skin samples were then treated through four different protocols: (i) Applying 200 mg of each commercial product (HA, AA, INK) individually. (ii) Pre-treatment with Dermapen® (1000 µm length, 8000 RPM) followed by the same quantity of each product. (iii) Initial application of the commercial products, then post-treatment with Dermapen®. (iv) Applying the alpha-arbutin-loaded PVPVA microneedles.

Post-permeation, excess product was wiped off the skin using sponges dampened with a 3% Teepol solution. The absorbed solution in sponges was collected for HPLC quantification as total skin wash. Formulation remnants in the donor chamber were also collected. The skin was then subjected to 15 consecutive tape strippings to remove the stratum corneum layers. Components from each step of the Franz cell process (skin wash, donor chamber wash, tape strips, and residues after stripping) were solubilized with a methanol and ultra-purified water mixture (30% methanol), agitated for 1 minute and sonicated for half an hour. Following this, 1 mL of each sample was extracted for HPLC assessment. Similarly, 1 mL of receptor fluid was also collected from each Franz cell for analysis. These samples were centrifuged at 14000 rpm at 4 $^{\circ}$ C for 10 minutes and filtered through a 0.22 µm filter for subsequent HPLC analysis.

2.4. Quantification of alpha-arbutin by HPLC

For the chromatographic analysis, a Hypersil BDS C18 column (150 mm in length and 4.6 mm in diameter with 3.0 µm particles) was employed. The operational flow rate was set to 0.5 mL per minute, and the injection volume was precisely 10.00 µL. We maintained the column temperature at a steady 30 °C. The UV detection

was programmed at a wavelength of 280 nm, and the emission wavelength was accordingly set. Each sample underwent a 20-minute analysis duration. A mobile phase consisting of acetate buffer (0.1 M, with a pH level of 4.0) and methanol in a 95:5 volume-to-volume ratio was utilized.

We evaluated the method's linearity across various concentrations, selecting twelve concentrations ranging from 0.1 to 1024 μg/mL. A calibration curve was plotted by correlating peak areas with the alpha-arbutin concentrations they represented. Through linear regression, we ascertained the slope, the y-intercept, and the correlation coefficient (R2) of the curve[44]. This yielded a formula expressing the relationship between the concentration and the area as $y = 0.0862x + 0.2359$, achieving a coefficient of determination of 0.9999.

In compliance with FDA guidelines[45], we calculated the method's theoretical limit of detection (LOD) and limit of quantification (LOQ). These were determined using the standard deviation of the response (σ) and the calibration curve's slope (S) through the equations: $LOD = 3.3\sigma/S$ and $LOQ = 10\sigma/S$. We found the LOD for alpha-arbutin to be 0.0646 μg/mL and the LOQ to be 0.1937 μg/mL. Thus, the established HPLC methodology is sufficiently sensitive for the quantification of alpha-arbutin in skin permeation studies within the tested concentration range.

2.5. Imaging analysis of alpha-arbutin within the skin by 3D OrbiSIMS

Selected skin specimens from the Franz cell investigations detailed in Section 2.1.2 were prepared for visual analysis. To clear any residual formula, the skin's

surface was cleansed using a damp sponge, followed by a dry one. The specimens were instantly subjected to a rapid freeze with liquid nitrogen to prevent morphological changes or autolytic damage. They were then mounted on a cryostat (Leica Biosystems, Wetzlar, Germany) for the creation of frozen sections (CT at -24 °C, OT at -30 °C), producing 20 µm thick cross-sections, placing three per slide. Adjacent sections of 20 µm thickness were set aside for conventional haematoxylin-eosin staining procedures.

Subsequently, the skin sections underwent 3D OrbiSIMS analysis (Hybrid SIMS, IONTOF GmbH, Germany). For Orbitrap imagery, we employed a 20 KeV $Ar3000^+$ ion beam, 20 µm in diameter, as the primary ion source. The analysis was conducted at ambient temperature over a 300 × 300 µm square area, using a negative polarity setting. The Ar3000+ ions were generated with a filament current of 2.30 A, while charge compensation was achieved with a -20 eV electron flood gun. The operational duty cycle was fixed at 4.4%, with a cycle duration of 200 µs. To assist in charge balancing, argon gas was flooded into the chamber to maintain a pressure of 9.0×10^{-7} mbar. The target surface potential was optimized to 136.6 V. We recorded mass spectra at a high resolution of 240,000 at m/z 200, across a mass range of 75 to 1,125 m/z. The AGC target was deactivated, setting the injection cap at 500 ms. Data collection and analysis were both carried out using SurfaceLab 7 software (IONTOF GmbH), with Orbitrap data collated via a Thermo Fisher Orbitrap HF mass spectrometer.

2.6. Statistical Analysis

Presented data reflect averages plus or minus the standard deviation, with sample sizes of three or more ($n \geq 3$). We utilized Prism 8 for statistical analyses. A one-way analysis of variance (ANOVA) was applied to ascertain significant differences, followed by Dunnett's multiple comparisons test as a post-hoc analysis for ANOVA. Significance levels are denoted as follows *, $p<0.05$; **, $p<0.01$.

3. Results and discussion

3.1. Formulation and fabrication of DMNs

Alpha-arbutin-loaded PVPVA DMNs were successfully fabricated using a two-step casting process as previously reported[46]. The rigidity of the needle tips was increased by the introduction of PEG 400. According to a previous report[46], the DMNs formed from PVPVA and PEG 400 materials have good mechanical strength and puncture capacity, so their properties will not be expanded on in detail here. The backing layer of the microneedles is flexible due to the combination of glycerol and CMC, and as such, demoulding is successfully manipulated.

The images of a top view and side view of the alpha-arbutin-loaded PVPVA DMNs are illustrated in **Figure. 1**a,b. **Figure. 1**c shows a side view image from an optical microscope of the alpha-arbutin-loaded PVPVA DMN with needle tip lengths of 1000 nm. As shown in **Figure. 1**d-g from scanning electron microscopy (SEM), the needles have an obelisk design with base widths of 284.2 µm and 276.1 µm. It can also be clearly seen that this is a 10×10 array of microneedles with a tip-to-tip spacing of 800 µm.

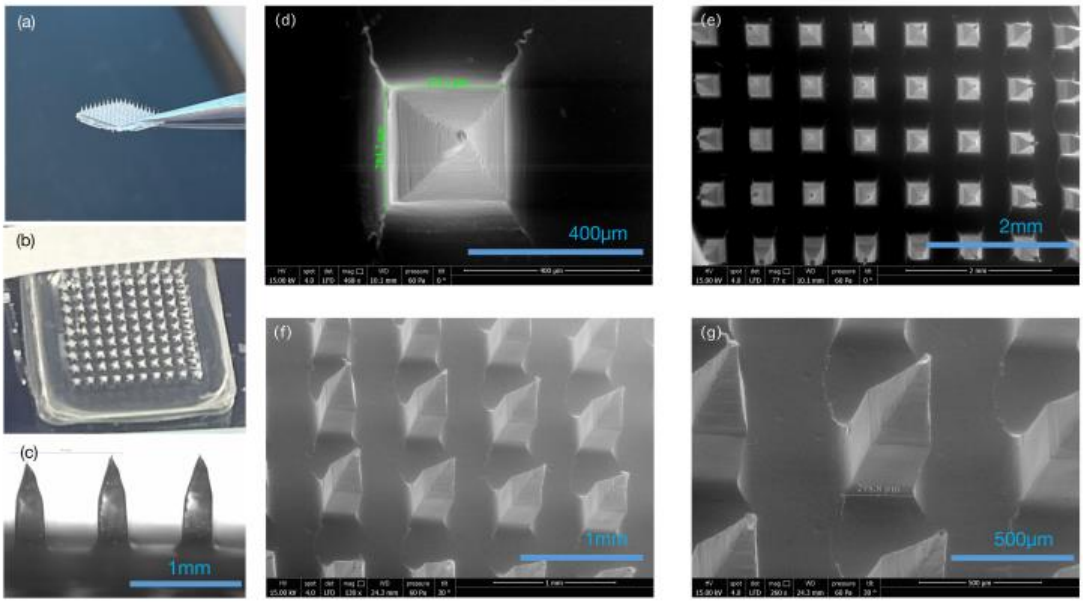

Figure 1. Images of alpha-arbutin-loaded PVPVA microneedle, from optical microscope (20x) (a) side view of 10 x10 array of microneedles (20x) (b) top view of 10 x10 array of microneedles (c) side view of individual microneedles(20x); from SEM images of alpha-arbutin-loaded PVPVA microneedle (d(468x)e(77x)) top view (f(130x)g(260x)) side view.

3.2. HPLC quantification of alpha-arbutin from the Franz cell component of the permeation study

3.2.1. Commercial alpha-arbutin products without and with Dermapen® pretreatment or posttreatment

The skin permeation of commercial alpha-arbutin products without Dermapen® in different Franz cell components following a 24-hour permeation test is illustrated in **Figure. 2**A and **Table S1**. Almost 99% of the alpha-Arbutin dosed was found in donor wash and skin wash compared to the other Franz cell components (**Table**

S1), indicating that the vast majority of alpha-Arbutin failed to penetrate the skin. Indeed, a limited amount of drug penetration into the skin was observed, with only approximately 0.4-1.1% of the active ingredient remaining in the skin. Additionally, less than 0.02% of alpha-arbutin for all three products was able to penetrate through the dermis to reach the receptor compartment (**Table S1**). Overall, we found that alpha-arbutin has limited permeation into the skin (tape strips and remaining in skin) and across the skin (receptor fluid). This can be attributed to the high hydrophilicity of alpha-arbutin, which makes it difficult to permeate through the hydrophobic stratum corneum, as also reported by Won et al.[47]. In Won's study, 2% alpha-arbutin resulted in 0.97 ± 1.76 μg/mL deposition in the epidermis and dermis, which was consistent with our results.

As shown in **Figure. 2**B, following application of Dermapen® as pretreatment, in comparison with permeation without Dermapen®, the mean percentage of alpha-arbutin remaining in the skin from the commercial products HA, AA, or INK was increased by approximately 1.5 times, 2.2 times, and 1.4 times, respectively (**Table S1**). The mean percentage of alpha-arbutin in the receptor fluid (across the skin) for HA, AA, and INK, shown in **Table S1**, although slightly increased, remained no more than 0.6% of the total dose administered.

The mean percentage of commercial alpha-arbutin products with the application of Dermapen® as posttreatment in different Franz cell components following the 24-hour permeation test is shown in **Figure. 2**C. Following Dermapen® posttreatment, in comparison to those without application of microneedles, the

mean percentage of alpha-arbutin from the commercial HA product in tape strips, remaining in skin, and receptor fluid was increased by approximately 9 times, 3 times and 30 times, respectively; the mean percentage of alpha-arbutin of the AA product in tape strips, remaining in skin and receptor fluid was increased by approximately 10 times, 14 times and 74 times, respectively; and the mean percentage of alpha-arbutin of the INK product in tape strips, remaining in skin, and receptor fluid was increased by approximately 6 times, 17 times and 261 times, respectively, indicating that the permeation into the skin (tape strips and remaining in skin) was largely improved (**Table S1**). Overall, this application provides a useful intradermal delivery system that can be more effective for alpha-arbutin to treat hyperpigmentation disorders. However, attention needs to be paid to the fact that the proportion permeated across skin into the receptor fluid was also increased in parallel, suggesting a potential increase in systemic exposure (**Table S1**).

3.2.2. Alpha-arbutin-loaded dissolving microneedles (DMNs)

The mean percentage of permeation of alpha-arbutin from alpha-arbutin-loaded PVPVA DMNs in different Franz cell components following the 24-hour permeation test is illustrated in **Figure. 2**D.

In this study, the drug concentration in the soluble microneedle was controlled to be 2% w/w, the same as that in commercial products. Following alpha-arbutin-loaded PVPVA microneedle application, the mean percentage of permeation of alpha-arbutin remaining in skin was a 6-fold increase compared to that without MN application (**Table S2**). This indicates that the permeation into the skin (tape strips and remaining in skin) was largely improved with this application. In addition, the

drug content of the receptor fluid (transdermal delivery) was also significantly higher, up to 1%, suggesting a potential increase in systemic exposure (**Table S1**).

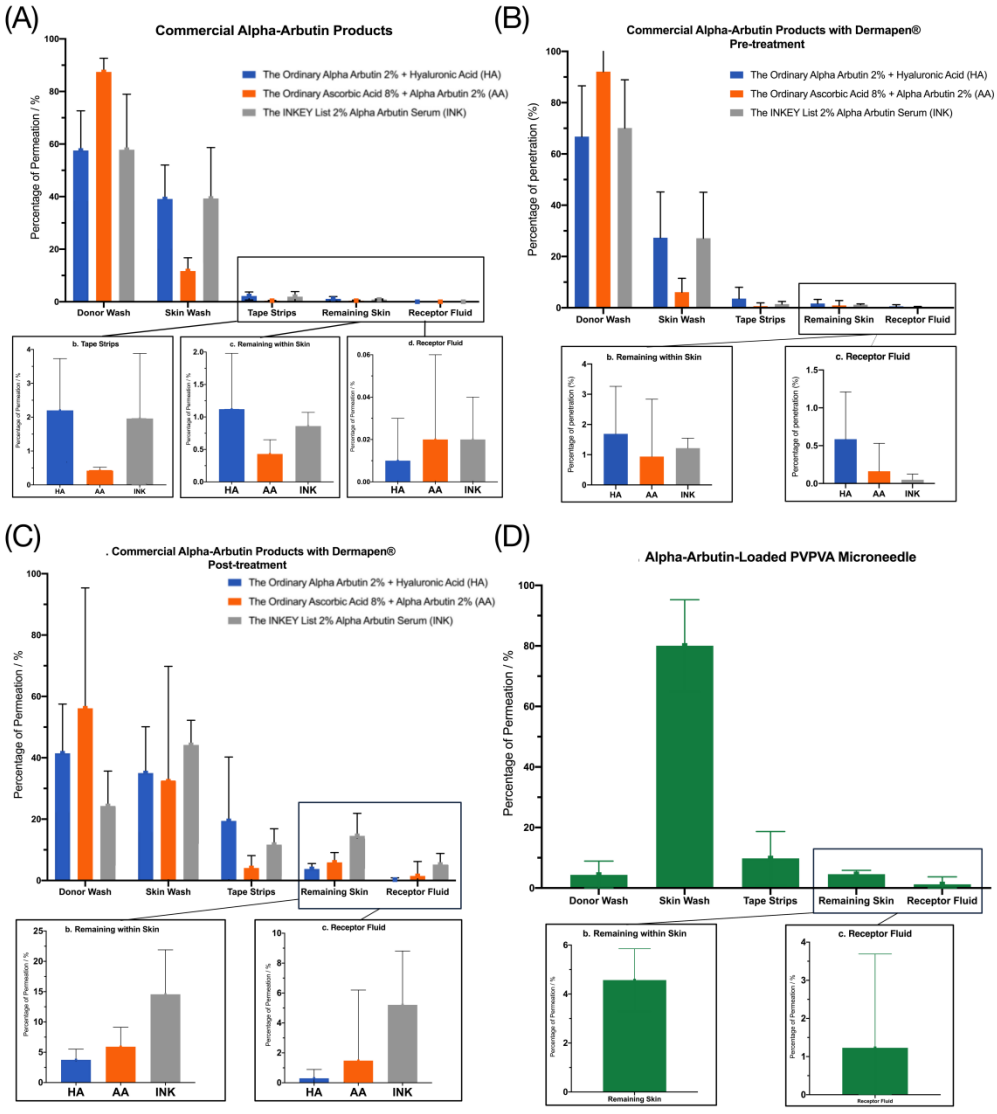

Figure 2. HPLC quantification of permeation of (A) commercial alpha-arbutin products, n=3; (B) commercial alpha-arbutin products with Dermapen® pretreatment, n=6; (C) commercial alpha-arbutin products with Dermapen® posttreatment, n=6; and (D) alpha-arbutin-loaded PVPVA microneedle application (n=4), in different Franz cell components (donor wash, skin wash, tape strips,

remaining skin and receptor fluid) following 24-hour permeation test. The inserts provide enlarged details on the permeation percentage of commercial alpha-arbutin products in (a) tape strips, remaining skin and receptor fluid, and (b-d) remaining skin and receptor fluid. The data are expressed as the means ± SDs (n≥3). HA stands for Ordinary® Alpha Arbutin 2% + Hyaluronic Acid; AA stands for Ordinary® Ascorbic Acid 8%+Alpha Arbutin 2%; INK stands for INKEY List® 2% Alpha Arbutin Serum.

3.3. Comparison between different applications and types of microneedles

Since alpha-arbutin targets melanocytes located within the basal layer of the skin, it is most important to confirm the amount of alpha-arbutin remaining in the skin. The statistical comparison for the permeation of alpha-arbutin into the remaining skin between pretreatment or posttreatment applications of Dermapen® (CMNs) or alpha-arbutin-loaded PVPVA microneedle (DMNs) and without any application of microneedles, shows that CMN pretreatment application does not significantly improve the permeation of alpha-arbutin. Interestingly and as expected, it was observed that CMN posttreatment produced a significantly higher permeation of alpha-arbutin in the formulation of HA, AA and INK products, similar to the DMN application, which also largely improved the permeation of alpha-arbutin, as summarized in **Figure. 3**.

Theoretically, the enhancement of skin permeation of alpha-arbutin should be more pronounced following the application of DMNs, as these microneedles allow for the complete loading and subsequent release of the drug into the skin tissue,

unlike CMNs, where a portion of the formulation might remain on the skin's surface. However, when comparing the percentage of alpha-arbutin permeation between treatments using Dermapen® CMNs and those utilizing alpha-arbutin-loaded PVPVA DMNs, no statistically significant difference in permeation was observed, as depicted in **Figure. 3**.

Although the permeation of alpha-arbutin with posttreatment application of Dermapen® is only slightly different compared with alpha-arbutin-loaded PVPVA DMNs, the standard deviation of the mean permeation for the Dermapen® application is much higher. This indicates that the results varied largely between each application[48], suggesting that this may be due to the drug loss caused by Dermapen® during application.

Normally, CMNs are used for skin pretreatment prior to drug application. However, it was discovered that the channels generated in the dermal layer of the skin usually immediately recoil and reseal after microneedle application[49]. Therefore, CMNs were used after drug application in this study. However, it was observed that a large amount of the formulation was left in the microneedle cartridge when CMNs were applied as posttreatment, as shown in **Figure. S**1. This leads to a large amount of formulation being wasted and reduces the permeation rate of the drug. Furthermore, as different formulations have different viscosities for the needle, the amount left in the cartridge is varied, as presented in **Figure S1** and **Table S3**. Therefore, if CMNs are to be utilized for reprocessing in the future, the formulation needs to be improved to decrease its likelihood of remaining inside the

cartridge. This also provides a reason to explore new delivery methods, such as dissolvable microneedles.

Since both CMNs and DMNs are able to pierce the outermost layer of skin and create microchannels reaching the depth of the dermal papillae, an increase in alpha-arbutin permeation into the receptor fluid was expected and observed. Higher amounts of alpha-arbutin bypassed the skin barriers through the created microchannels and were present in the receptor fluid[50]. However, these results were not as we hoped, as the excessive amount of alpha-arbutin that crosses the skin may enter the blood circulation. Overall, CMNs posttreatment had a higher transdermal delivery rate than DMNs (**Table S1**).

In summary, from the comparison of the permeation of alpha-arbutin remaining in skin following the three treatment modalities, as illustrated in **Figure. 3**, microneedles in general improve the permeation of alpha-arbutin into the skin; in particular, DMNs offer the best prospects in terms of patient compliance and safety.

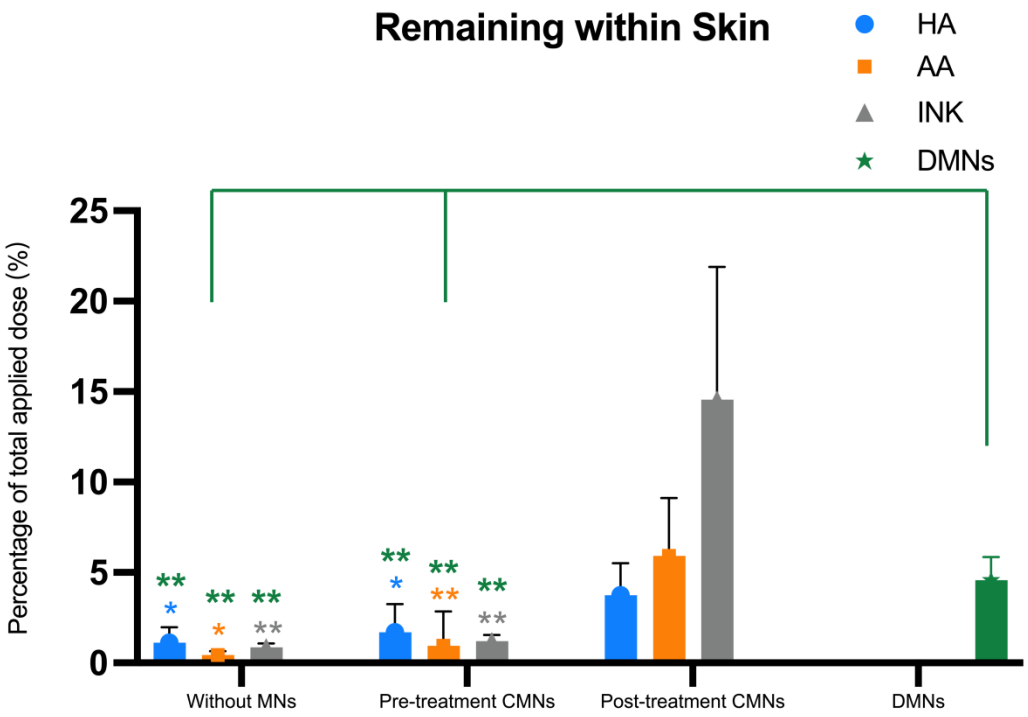

Figure 3. HPLC analysis of alpha-arbutin remaining in skin without microneedles (MNs), with Dermapen® pre/post treatment (CMNs) and with alpha-arbutin-loaded PVPVA microneedles (DMNs) after a 24-hour permeation test. The data are expressed as the means ± SDs (n≥3). One-way ANOVA was used to determine statistical significance (*$p < 0.05$; **$p < 0.01$; no significant difference (ns) $p > 0.05$). The green asterisks indicate a comparison to DMNs, while the blue (HA), orange (AA) and grey (INK) asterisks signify comparisons to posttreatment CMNs.

3.4. Visualization of alpha-arbutin within the skin by 3D OrbiSIMS

Although the use of HPLC analysis provides useful insights into the quantifiable permeation of compounds within the skin, it is unable to provide more precise information on visible locations on specific skin layers. Therefore, using skin

sections in combination with 3D OrbiSIMS imaging was explored to investigate the depth distribution of alpha-arbutin within the skin.

Before conducting imaging analysis using 3D OrbiSIMS, the secondary ions underwent preliminary analysis using an Orbitrap analyser. This step aimed to generate 3D OrbiSIMS negative polarity depth profiles, which were essential for identifying distinct markers suitable for localizing different skin layers (**Figure. 4** a-c). Subsequently, as depicted in **Figure. 4**d-e, the successful detection of the active ingredient was confirmed. Notably, this analysis revealed the absence of any interfering peaks within the selected peak segments.

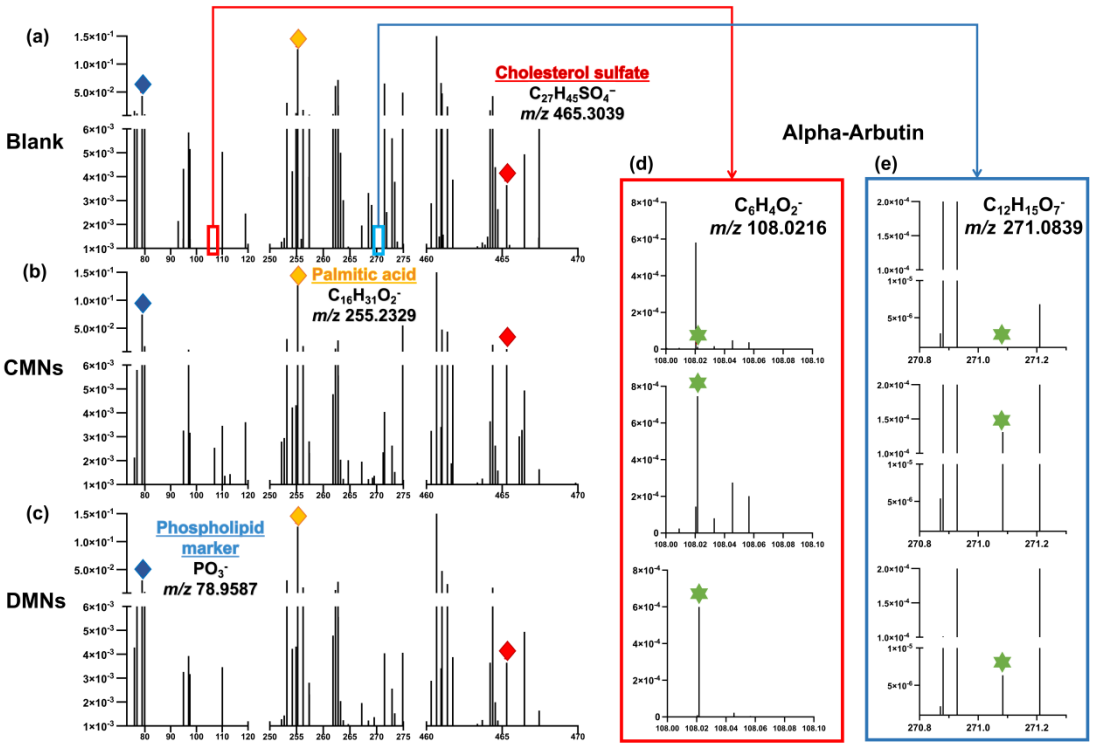

Figure. 4. 3D OrbiSIMS negative polarity depth profile spectrum. (a) The ion spectrum of the blank group dosed with ultra-purified water. (b) The ion spectrum

of CMNs treated with the commercial alpha-arbutin product (HA) and Dermapen® posttreatment. (c) The ion spectrum of DMNs dosed by alpha-arbutin-loaded PVPVA microneedles. The spectrum presents the total ion intensity for the 300 μm ×300 μm area and is labelled with (Blue) phospholipid marker (PO_3^-), (Yellow) palmitic acid ($C_{16}H_{31}O_2^-$), and (Red) cholesterol sulfate ($C_{27}H_{45}SO_4^-$) as skin markers. (d) The ion spectrum of the alpha-arbutin fragment ($C_6H_4O_2^-$) in the blank, CMN, and DMN groups. (e) The ion spectrum of alpha-arbutin ($C_{12}H_{15}O_7^-$) in the blank, CMN, and DMN groups.

Due to the variation in pig skin thickness, it is important to identify the thickness of the epidermis based on sections from the adjacent site. For example, **Figure. 5**A shows that the thickness of the stratum corneum at this site is 10-15 μm, and the thickness of the epidermis is 20-150 μm. Melanocytes containing tyrosinase are located between the epidermis and the dermis in a structure with only one layer of cells, located approximately 150-160 μm from the surface of the skin.

As reported by Nichola N et al.[51]., palmitic acid ($C_{16}H_{31}O_2^-$) and cholesterol sulfate ($C_{27}H_{45}SO_4^-$) can be used to localize the uppermost layers of the stratum corneum and epidermis. Alternatively, PO_3^-, which is usually found in the epidermis and dermis, can also be used to help with localization, as shown in **Figure. 5**B. In our study, high-intensity Arbutin fragment ions were detectable by OrbiSIMS analysis, with the fragment molecular ion of Arbutin ($C_{12}H_{16}O_7$) being $C_{12}H_{15}O_7^-$ (**Figure. 5**B). Clearly, most of the Arbutin in the DMNs group is cleaved into fragments by the electron flood gun. The ion $C_6H_4O_2^-$ (**Figure. 5**B) was found to

have a significant signal intensity in both samples, while it was barely visible in the blank skin group, indicating that $C_6H_4O_2^-$ is an exogenous substance and is not part of the ionic signal fragment present in the skin itself. A logical inference is that $C_6H_4O_2^-$ could be used as a representative ionic fragment of alpha-arbutin and as a marker for the localized compound.

The ability to enhance the intradermal accessibility of alpha-arbutin using CMN or DMN augmentation requires further definitive localization. As seen in **Figure. 5**C(a), the alpha-arbutin fragment signal overlaps substantially with molecular ion cholesterol sulfate ($C_{27}H_{45}SO_4^-$) with posttreatment application of CMNs, indicating that it mainly accumulates in the stratum corneum and upper epidermis and does not enter deeper parts of the skin. In contrast, the ionic signal of alpha-arbutin (green) in **Figure. 5**C(b) clearly appears below the stratum corneum with the application of DMNs. It overlaps with the position of the PO_3^- ion, indicating that it is distributed in the epidermis and mainly accumulates in the lower epidermal layers where melanocytes reside as the target site. Thus, the images reveal the molecular mechanism for the targeted delivery of DMNs that have a significantly enhanced effect on the permeation of this compound.

We attribute this outcome to the selection of polymeric DMNs. Compared to the typical DMN, the polymeric DMN offers ease of construction and significantly enhances the transdermal delivery efficiency of the encapsulated compounds[52]. Among the many different polymeric materials, PVPVA was chosen because of its excellent biocompatibility and hydrophilicity. Notably, alpha-arbutin, a hydrophilic

active pharmaceutical ingredient (API), can be dissolved in an aqueous medium together with PVPVA for easy formulation and release. Moreover, it has been demonstrated that PVPVA-based DMNs have good hygroscopicity and intradermal dissolubility[53]. Thus, PVPVA-based DMNs are sufficiently permeable to dissolve rapidly in the epidermis, leading to efficient drug penetration. In addition, according to a recently published study[46], PVPVA was developed to make DMNs for the treatment of basal cell carcinoma (BCC) with excellent targeting to the skin basal layer. Therefore, PVPVA-based DMNs can improve the targeted delivery of alpha-arbutin to the basal layer.

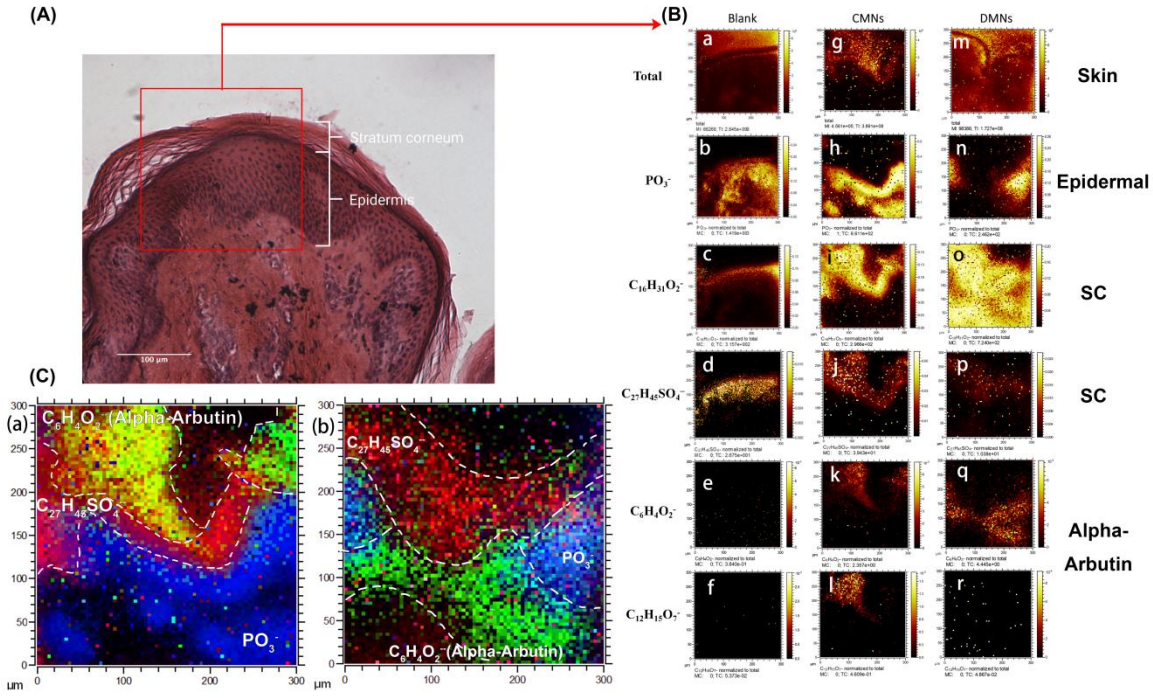

Figure. 5. Images of full thickness porcine skin tissue (4 mm). (A) HE-stained cross-section of DMN-dosed skin tissue. The epidermal thickness of the skin sample is labelled on the image. Image from 20 μm Cryocut tissue sections at a

10-fold magnification. **(B)** Negative polarity ion images of 3D OrbiSIMS from various fragment ions of the skin cross-section dosed by alpha-arbutin-loaded PVPVA microneedles (DMNs) and commercial alpha-arbutin products with Dermapen® posttreatment (CMNs), while ultra-purified water was used as a blank group. The field of view is 300.0 µm, and the pixel size is 4.0 µm. MC stands for the maximum ion count per pixel, and TC is the total ion count for the specific ion of interest. The ion images illustrate the 2D spatial distribution for the following molecular ions: (a, g, m) total ions; (b, h, n) phospholipid marker (PO_3^-); (c, i, o) palmitic acid ($C_{16}H_{31}O_2^-$); (d, j, p) cholesterol sulfate ($C_{27}H_{45}SO_4^-$); (e, k, q) alpha-arbutin fragment ($C_6H_4O_2$-); and (a-f) blank group, (g-l) CMN group, and (m-r) DMN group. All ion images were normalized to the total ion counts. **(C)** Images of 3D OrbiSIMS from various fragment ions overlaid on the skin cross-section dosed by commercial alpha-arbutin products with (a) Dermapen® posttreatment and (b) alpha-arbutin-loaded PVPVA microneedles. The Field of View: 300.0 µm and Pixelsize: 4.0 µm. The ion images illustrate the 2D spatial distribution for the overlay of different molecular ions. Three color overlays between ion images; stratum corneum and top of epidermis (cholesterol sulfate fragment, $C_{27}H_{45}SO_4^-$, red), epidermis (phospholipid marker, PO_3^-, blue) and alpha-arbutin fragment ($C_6H_4O_2^-$, green).

4. CONCLUSIONS

The permeation of alpha-arbutin through the skin from three different commercial products was first evaluated. In the absence of microneedles, a low permeation of alpha-arbutin was observed due to its high hydrophilicity.

Both solid steel microneedle posttreatment and dissolving polymeric microneedles loaded with alpha-arbutin largely improved alpha-arbutin skin permeation, as demonstrated by HPLC analysis. Furthermore, the combination of 3D OrbiSIMS and skin cross-section analysis was used for the first time to visualize the distribution and localization of alpha-arbutin within the skin by the high-resolution imaging technique, demonstrating the effectiveness of dissolving polymeric microneedles in improving the permeation of alpha-arbutin and specifically targeting the epidermal junction where melanocytes reside. Overall, this demonstrates that dissolving polymeric microneedles are more effective than solid steel microneedles at reaching the target site. Moreover, in terms of compliance and safety, dissolving polymeric microneedles offers much better prospects. Thus, this study suggests that dissolving polymeric microneedles are a promising delivery system to facilitate targeted intradermal delivery of alpha-arbutin.

REFERENCES

[1] M. Brenner, V.J. Hearing, The Protective Role of Melanin Against UV Damage in Human Skin†, Photochemistry and Photobiology. 84 (2008) 539–549. https://doi.org/10.1111/j.1751-1097.2007.00226.x.

[2] E. Nicolaidou, A.D. Katsambas, Pigmentation disorders: hyperpigmentation and hypopigmentation, Clinics in Dermatology. 32 (2014) 66–72. https://doi.org/10.1016/j.clindermatol.2013.05.026.

[3] Quality of life in dermatology - Halioua - 2000 - International Journal of Dermatology - Wiley Online Library, (n.d.). https://onlinelibrary.wiley.com/doi/full/10.1046/j.1365-4362.2000.00793.x?casa_token=-PoIQ2zd-38AAAAA%3ADMJHqNN6uvOEut6_yqQeuwJw9oveonoi0_5L6AI_fcgRZIAJWqm6WcIsgWlgGm0dEOk4K3x9RZ4qOA (accessed October 30, 2022).

[4] M. Kanlayavattanakul, N. Lourith, Plants and Natural Products for the Treatment of Skin Hyperpigmentation – A Review, Planta Med. 84 (2018) 988–1006. https://doi.org/10.1055/a-0583-0410.

[5] S. Briganti, E. Camera, M. Picardo, Chemical and Instrumental Approaches to Treat Hyperpigmentation, Pigment Cell Research. 16 (2003) 101–110. https://doi.org/10.1034/j.1600-0749.2003.00029.x.

[6] S. Plensdorf, M. Livieratos, N. Dada, Pigmentation Disorders: Diagnosis and Management, Am Fam Physician. 96 (2017) 797–804.

[7] T. Pillaiyar, V. Namasivayam, M. Manickam, S.-H. Jung, Inhibitors of Melanogenesis: An Updated Review, J. Med. Chem. 61 (2018) 7395–7418. https://doi.org/10.1021/acs.jmedchem.7b00967.

[8] K. Sugimoto, T. Nishimura, K. Nomura, K. Sugimoto, T. Kuriki, Syntheses of Arbutin-α-glycosides and a Comparison of Their Inhibitory Effects with Those of α-Arbutin and Arbutin on Human Tyrosinase, Chemical and Pharmaceutical Bulletin. 51 (2003) 798–801. https://doi.org/10.1248/cpb.51.798.

[9] C. j. Morgan, A. g. Renwick, P. s. Friedmann, The role of stratum corneum and dermal microvascular perfusion in penetration and tissue levels of water-soluble drugs investigated by microdialysis, British Journal of Dermatology. 148 (2003) 434–443. https://doi.org/10.1046/j.1365-2133.2003.05163.x.

[10] Y. Naoe, T. Hata, K. Tanigawa, H. Kimura, T. Masunaga, Bidimensional analysis of desmoglein 1 distribution on the outermost corneocytes provides the structural and functional information of the stratum corneum, Journal of Dermatological Science. 57 (2010) 192–198. https://doi.org/10.1016/j.jdermsci.2009.12.014.

[11] M. Akiyama, Corneocyte lipid envelope (CLE), the key structure for skin barrier function and ichthyosis pathogenesis, Journal of Dermatological Science. 88 (2017) 3–9. https://doi.org/10.1016/j.jdermsci.2017.06.002.

[12] M.R. Prausnitz, P.M. Elias, T.J. Franz, M. Schmuth, J.-C. Tsai, G.K. Menon, W.M. Holleran, K.R. Feingold, 124 Skin Barrier and Transdermal Drug Delivery, (n.d.) 10.

[13] F. Pati, B. Adhikari, S. Dhara, Development of chitosan–tripolyphosphate fibers through pH dependent ionotropic gelation, Carbohydrate Research. 346 (2011) 2582–2588. https://doi.org/10.1016/j.carres.2011.08.028.

[14] N. Chandorkar, S. Tambe, P. Amin, C. Madankar, Alpha Arbutin as a Skin Lightening Agent: A Review, 13 (2021) 3502–3510. https://doi.org/10.31838/ijpr/2021.13.02.446.

[15] S.H. Bariya, M.C. Gohel, T.A. Mehta, O.P. Sharma, Microneedles: an emerging transdermal drug delivery system, Journal of Pharmacy and Pharmacology. 64 (2012) 11–29.

[16] M.S. Roberts, Y. Mohammed, M.N. Pastore, S. Namjoshi, S. Yousef, A. Alinaghi, I.N. Haridass, E. Abd, V.R. Leite-Silva, H.A.E. Benson, Topical and cutaneous delivery using nanosystems, Journal of Controlled Release. 247 (2017) 86–105.

[17] T. Hong, W. Liu, M. Li, C. Chen, Recent advances in the fabrication and application of nanomaterial-based enzymatic microsystems in chemical and biological sciences, Analytica Chimica Acta. 1067 (2019) 31–47.

[18] S.Z. Razzacki, P.K. Thwar, M. Yang, V.M. Ugaz, M.A. Burns, Integrated microsystems for controlled drug delivery, Advanced Drug Delivery Reviews. 56 (2004) 185–198.

[19] V. Van Tran, T.L. Nguyen, J.-Y. Moon, Y.-C. Lee, Core-shell materials, lipid particles and nanoemulsions, for delivery of active anti-oxidants in cosmetics applications: Challenges and development strategies, Chemical Engineering Journal. 368 (2019) 88–114.

[20] K. Maaden, W. Jiskoot, J. Bouwstra, Microneedle technologies for (trans)dermal drug and vaccine delivery, Journal of Controlled Release. 161 (2012) 645–655. https://doi.org/10.1016/j.jconrel.2012.01.042.

[21] R.F. Donnelly, D.I. Morrow, P.A. McCarron, A.D. Woolfson, A. Morrissey, P. Juzenas, A. Juzeniene, V. Iani, H.O. McCarthy, J. Moan, Microneedle-mediated intradermal delivery of 5-aminolevulinic acid: potential for enhanced topical photodynamic therapy, Journal of Controlled Release. 129 (2008) 154–162.

[22] J.-H. Oh, H.-H. Park, K.-Y. Do, M. Han, D.-H. Hyun, C.-G. Kim, C.-H. Kim, S.S. Lee, S.-J. Hwang, S.-C. Shin, Influence of the delivery systems using a microneedle array on the permeation of a hydrophilic molecule, calcein, European Journal of Pharmaceutics and Biopharmaceutics. 69 (2008) 1040–1045.

[23] Y.-C. Kim, J.-H. Park, M.R. Prausnitz, Microneedles for drug and vaccine delivery, Advanced Drug Delivery Reviews. 64 (2012) 1547–1568. https://doi.org/10.1016/j.addr.2012.04.005.

[24] T.-M. Tuan-Mahmood, M.T.C. McCrudden, B.M. Torrisi, E. McAlister, M.J. Garland, T.R.R. Singh, R.F. Donnelly, Microneedles for intradermal and transdermal drug delivery, European Journal of Pharmaceutical Sciences. 50 (2013) 623–637. https://doi.org/10.1016/j.ejps.2013.05.005.

[25] M.H. Al-Mayahy, A.H. Sabri, C.S. Rutland, A. Holmes, J. McKenna, M. Marlow, D.J. Scurr, Insight into imiquimod skin permeation and increased delivery using microneedle pre-treatment, European Journal of Pharmaceutics and Biopharmaceutics. 139 (2019) 33–43. https://doi.org/10.1016/j.ejpb.2019.02.006.

[26] T. Waghule, G. Singhvi, S.K. Dubey, M.M. Pandey, G. Gupta, M. Singh, K. Dua, Microneedles: A smart approach and increasing potential for transdermal drug delivery system, Biomedicine & Pharmacotherapy. 109 (2019) 1249–1258. https://doi.org/10.1016/j.biopha.2018.10.078.

[27] S. Bal, A. c. Kruithof, H. Liebl, M. Tomerius, J. Bouwstra, J. Lademann, M. Meinke, In vivo visualization of microneedle conduits in human skin using laser scanning microscopy, Laser Physics Letters. 7 (2010) 242–246. https://doi.org/10.1002/lapl.200910134.

[28] A. Sabri, J. Ogilvie, J. McKenna, J. Segal, D. Scurr, M. Marlow, Intradermal Delivery of an Immunomodulator for Basal Cell Carcinoma; Expanding the Mechanistic Insight into Solid Microneedle-Enhanced Delivery of Hydrophobic Molecules, Mol. Pharmaceutics. 17 (2020) 2925–2937. https://doi.org/10.1021/acs.molpharmaceut.0c00347.

[29] X. He, J. Sun, J. Zhuang, H. Xu, Y. Liu, D. Wu, Microneedle System for Transdermal Drug and Vaccine Delivery: Devices, Safety, and Prospects, Dose-Response. 17 (2019) 1559325819878585. https://doi.org/10.1177/1559325819878585.

[30] K.N. Mangang, P. Thakran, J. Halder, K.S. Yadav, G. Ghosh, D. Pradhan, G. Rath, V.K. Rai, PVP-microneedle array for drug delivery: mechanical insight, biodegradation, and recent advances, Journal of Biomaterials Science, Polymer Edition. 34 (2023) 986–1017. https://doi.org/10.1080/09205063.2022.2155778.

[31] Y. Park, J. Park, G.S. Chu, K.S. Kim, J.H. Sung, B. Kim, Transdermal delivery of cosmetic ingredients using dissolving polymer microneedle arrays, Biotechnology and Bioprocess Engineering. 20 (2015) 543–549.

[32] F.K. Aldawood, A. Andar, S. Desai, A Comprehensive Review of Microneedles: Types, Materials, Processes, Characterizations and Applications, Polymers. 13 (2021) 2815. https://doi.org/10.3390/polym13162815.

[33] N.N. Aung, T. Ngawhirunpat, T. Rojanarata, P. Patrojanasophon, P. Opanasopit, B. Pamornpathomkul, HPMC/PVP Dissolving Microneedles: a Promising Delivery Platform to Promote Trans-Epidermal Delivery of Alpha-Arbutin for Skin Lightening, AAPS PharmSciTech. 21 (2019) 25. https://doi.org/10.1208/s12249-019-1599-1.

[34] N.N. Aung, T. Ngawhirunpat, T. Rojanarata, P. Patrojanasophon, B. Pamornpathomkul, P. Opanasopit, Fabrication, characterization and comparison of α-arbutin loaded dissolving and hydrogel forming microneedles, International Journal of Pharmaceutics. 586 (2020) 119508. https://doi.org/10.1016/j.ijpharm.2020.119508.

[35] A.M. Judd, D.J. Scurr, J.R. Heylings, K.-W. Wan, G.P. Moss, Distribution and Visualisation of Chlorhexidine Within the Skin Using ToF-SIMS: A Potential Platform for the Design of More Efficacious Skin Antiseptic Formulations, Pharm Res. 30 (2013) 1896–1905. https://doi.org/10.1007/s11095-013-1032-5.

[36] M. Okamoto, N. Tanji, Y. Katayama, J. Okada, TOF-SIMS investigation of the distribution of a cosmetic ingredient in the epidermis of the skin, Applied Surface Science. 252 (2006) 6805–6808. https://doi.org/10.1016/j.apsusc.2006.02.218.

[37] C. Kern, R. Jamous, T.E. Khassawna, M. Rohnke, Characterisation of Sr 2+ mobility in osteoporotic rat bone marrow by cryo-ToF-SIMS and cryo-OrbiSIMS, Analyst. 147 (2022) 4141–4157. https://doi.org/10.1039/D2AN00913G.

[38] P. Agüi-Gonzalez, S. Jähne, N.T. N. Phan, SIMS imaging in neurobiology and cell biology, Journal of Analytical Atomic Spectrometry. 34 (2019) 1355–1368. https://doi.org/10.1039/C9JA00118B.

[39] M.K. Passarelli, A. Pirkl, R. Moellers, D. Grinfeld, F. Kollmer, R. Havelund, C.F. Newman, P.S. Marshall, H. Arlinghaus, M.R. Alexander, A. West, S. Horning, E. Niehuis, A. Makarov, C.T. Dollery, I.S. Gilmore, The 3D OrbiSIMS—label-free metabolic imaging with subcellular lateral resolution and high mass-resolving power, Nature Methods. 14 (2017) 1175–1183. https://doi.org/10.1038/nmeth.4504.

[40] A.M. Kotowska, G.F. Trindade, P.M. Mendes, P.M. Williams, J.W. Aylott, A.G. Shard, M.R. Alexander, D.J. Scurr, Protein identification by 3D OrbiSIMS to facilitate in situ imaging and depth profiling, Nat Commun. 11 (2020) 5832. https://doi.org/10.1038/s41467-020-19445-x.

[41] S. Xue, Z. Li, X. Ze, X. Wu, C. He, W. Shuai, M. Marlow, J. Chen, D. Scurr, Z. Zhu, J. Xu, S. Xu, Design, Synthesis, and Biological Evaluation of Novel Hybrids Containing Dihydrochalcone as Tyrosinase Inhibitors to Treat Skin Hyperpigmentation, J. Med. Chem. 66 (2023) 5099–5117. https://doi.org/10.1021/acs.jmedchem.3c00012.

[42] T.J. Franz, Percutaneous Absorption. On the Relevance of in Vitro Data, Journal of Investigative Dermatology. 64 (1975) 190–195. https://doi.org/10.1111/1523-1747.ep12533356.

[43] D.J. Davies, R.J. Ward, J.R. Heylings, Multi-species assessment of electrical resistance as a skin integrity marker for in vitro percutaneous absorption studies, Toxicology in Vitro. 18 (2004) 351–358. https://doi.org/10.1016/j.tiv.2003.10.004.

[44] G.A. Shabir, Validation of high-performance liquid chromatography methods for pharmaceutical analysis: Understanding the differences and similarities between validation requirements of the US Food and Drug Administration, the US Pharmacopeia and the

International Conference on Harmonization, Journal of Chromatography A. 987 (2003) 57–66. https://doi.org/10.1016/S0021-9673(02)01536-4.

[45] C. for D.E. and Research, Analytical Procedures and Methods Validation for Drugs and Biologics, U.S. Food and Drug Administration. (2020). https://www.fda.gov/regulatory-information/search-fda-guidance-documents/analytical-procedures-and-methods-validation-drugs-and-biologics (accessed October 30, 2022).

[46] A.H. Sabri, Z. Cater, P. Gurnani, J. Ogilvie, J. Segal, D.J. Scurr, M. Marlow, Intradermal delivery of imiquimod using polymeric microneedles for basal cell carcinoma, International Journal of Pharmaceutics. 589 (2020) 119808. https://doi.org/10.1016/j.ijpharm.2020.119808.

[47] J. Won, J.W. Park, Improvement of arbutin trans-epidermal delivery using radiofrequency microporation, Tropical Journal of Pharmaceutical Research. 13 (2014) 1775–1781. https://doi.org/10.4314/tjpr.v13i11.1.

[48] M.P. Barde, P.J. Barde, What to use to express the variability of data: Standard deviation or standard error of mean?, Perspect Clin Res. 3 (2012) 113–116. https://doi.org/10.4103/2229-3485.100662.

[49] J. Gupta, H.S. Gill, S.N. Andrews, M.R. Prausnitz, Kinetics of skin resealing after insertion of microneedles in human subjects, Journal of Controlled Release. 154 (2011) 148–155. https://doi.org/10.1016/j.jconrel.2011.05.021.

[50] J. Yang, X. Liu, Y. Fu, Y. Song, Recent advances of microneedles for biomedical applications: drug delivery and beyond, Acta Pharmaceutica Sinica B. 9 (2019) 469–483. https://doi.org/10.1016/j.apsb.2019.03.007.

[51] N.J. Starr, M.H. Khan, M.K. Edney, G.F. Trindade, S. Kern, A. Pirkl, M. Kleine-Boymann, C. Elms, M.M. O'Mahony, M. Bell, M.R. Alexander, D.J. Scurr, Elucidating the molecular landscape of the stratum corneum, Proceedings of the National Academy of Sciences. 119 (2022) e2114380119. https://doi.org/10.1073/pnas.2114380119.

[52] Z. Karim, P. Karwa, S.R.R. Hiremath, Polymeric microneedles for transdermal drug delivery-a review of recent studies, Journal of Drug Delivery Science and Technology. (2022) 103760.

[53] R. Parhi, Recent advances in microneedle designs and their applications in drug and cosmeceutical delivery, Journal of Drug Delivery Science and Technology. 75 (2022) 103639. https://doi.org/10.1016/j.jddst.2022.103639.

ASSOCIATED CONTENT

Supporting information

Figure S1. Photograph of drug residue remaining on the needle of Dermapen® after posttreatment of CMNs.

Table S1. HPLC analysis of mean alpha-arbutin from different Franz cell components, receptor fluid (RF), donor wash (DW), skin wash (SW), tape strips (TS) and remaining skin (RS) following a 24-hour permeation test by WMNs, CMNs and DMNs. The data are expressed as the means ± SDs (n≥3).

Franz Cell Components	Percentage (%) of alpha-arbutin in total dose administered									
	Commercial Alpha-Arbutin Products			Commercial Alpha-Arbutin Products with Dermapen® Pretreatment			Commercial Alpha-Arbutin Products with Dermapen® Posttreatment			Alpha-Arbutin-Loaded PVPVA Microneedle
	HA	AA	INK	HA	AA	INK	HA	AA	INK	2% w/w Alpha-Arbutin
Donor Wash	57.53±15.12	87.43±5.19	57.84±21.14	66.78±19.79	92.12±8.92	70.11±18.83	41.46±16.04	56.13±39.23	24.31±11.37	4.34±4.55
Skin Wash	39.12±12.90	11.68±5.06	39.29±19.40	27.36±17.82	6.1±5.42	27.16±17.92	35.03±15.07	32.35±37.46	44.19±8.04	80.04±15.22
Tape Strips	2.20±1.53	0.42±0.10	1.96±1.92	3.59±4.41	0.67±1.26	1.47±1.01	19.44±20.80	4.09±4.03	11.71±5.16	9.79±8.88
Remaining in Skin	1.12±0.86	0.43±0.22	0.86±0.21	1.69±1.57	0.94±1.9	1.22±0.33	3.75±1.76	5.91±3.21	14.56±7.34	4.57±1.28
Receptor Fluid	0.01±0.02	0.02±0.04	0.02±0.02	0.59±0.62	0.16±0.37	0.05±0.08	0.30±0.59	1.48±4.72	5.21±3.60	1.23±2.46

Table S2. HPLC analysis summary of alpha-arbutin permeation rates from remaining within skin of 24 h permeation test on different formulations with and without microneedles. The data are expressed as the means ± SDs (n≥3).

Percentage (%)	HA	AA	INK
Without MNs	1.12±0.86	0.43±0.22	0.86±0.21
CMNs pretreatment	1.69±1.57	0.94±1.90	1.22±0.33
CMNs posttreatment	3.75±1.76	5.91±3.21	14.56±7.34
		Alpha-Arbutin	
DMNs		4.57±1.28	

Table S3. HPLC analysis of permeation of commercial alpha-arbutin products(Administration Dose: 4000μg) with Dermapen® posttreatment, comparing the amount of alpha-arbutin between remaining on needle and collection from all franz cell components, following a 24-hour permeation test. The data are expressed as the means ± SDs (n≥6).

Amount (μg)	Remaining on needle(μg)	Collection from all franz cell components(μg)	Total amount(μg)	Recovery rate (%)
HA	1348.23±324.2	1419.25±575.45	2767.47±644.18	69.19±16.1
AA	2362.96±501.73	1503.59±1263.54	3882.69±1221.74	97.07±30.54
INK	2842.43±200.79	1239.11±744.14	3870.67±811.41	96.77±20.29